

PAPER

MIR plasmonic liquid sensing in nano-metric space driven by capillary force

To cite this article: Kailing Shih *et al* 2019 *J. Phys. D: Appl. Phys.* **52** 394001

View the [article online](#) for updates and enhancements.



IOP | ebooksTM

Bringing you innovative digital publishing with leading voices
to create your essential collection of books in STEM research.

Start exploring the collection - download the first chapter of
every title for free.

MIR plasmonic liquid sensing in nano-metric space driven by capillary force

Kailing Shih^{1,2,3}, Zhihao Ren^{1,2,3}, Chen Wang^{1,4} and Chengkuo Lee^{1,2,3,5,6} 

¹ Department of Electrical and Computer Engineering, National University of Singapore, 117576, Singapore

² Center for Intelligent Sensors and MEMS (CISM), National University of Singapore, 117608, Singapore

³ NUS Suzhou Research Institute (NUSRI), Suzhou, Industrial Park, Suzhou 215123, People's Republic of China

⁴ College of Biosystems Engineering and Food Science, Zhejiang University, Hangzhou 310058, People's Republic of China

⁵ Graduate School for Integrative Science and Engineering, National University of Singapore, Singapore

E-mail: elelc@nus.edu.sg

Received 25 February 2019, revised 4 June 2019

Accepted for publication 2 July 2019

Published 23 July 2019



Abstract

Optical spectroscopy in the mid-infrared region (MIR) has been an important tool for non-destructive analysis of molecules through identifying the vibrational modes of chemical bonds. The use of plasmonic antenna array in the MIR region enables high selectivity and sensitivity without the labeling process. In addition, the formation of nanogap between plasmonic nano-antenna and reflective mirror allows for near-field enhancement which can be exploited for sensing applications. However, it is still challenging to realize a sensing platform which effectively delivers biochemical molecules onto the plasmonic nanogap hot-spot.

Here, we experimentally demonstrate a capillary driven sensing platform confining chemical samples into a nano-metric space with a plasmonic antenna array. The quadrupole mode resonance of the plasmonic antenna combined with vertical nanogap hot-spot significantly enhanced the confined electrical field. The nano-metric spaces formed by hydrophilic silicon dioxide draw liquids into the sensing chamber by capillary effect, and hence no external liquid driving power source was required. Enhancement of both molecular vibration and plasmonic resonance were observed. Furthermore, label-free quantitative detection was achieved through coupling the plasmonic antenna resonance and the water molecular vibration. The proposed sensing platform has the potential in realizing non-destructive and label-free sensing in the MIR spectral region without an external liquid driving power source, and the enhanced signal paves the way to sense analyte of ultralow concentration.

Keywords: plasmonics, mid-infrared, capillary force, sensor

(Some figures may appear in colour only in the online journal)

1. Introduction

Optical spectroscopy is a powerful method enabling the analytical study of biochemical molecules in a non-destructive way [1–3]. In particular, the mid-infrared (MIR) spectral region (2–10 μm) is considered an important region because the incident light can directly excite the vibrational modes of

molecular bonds in biochemical samples [4–8]. Hence, identification of molecular fingerprint can be achieved without the labeling process in a non-destructive manner [9–12]. Despite the advantages that MIR spectroscopy provides in the detection of biochemical samples, the weak interaction between the incident light and the molecular vibrational modes leads to low absorption/scattering cross sections [13]. This limits the sensitivity and thus prevents the application of vibrational spectroscopies to practical use. One solution is utilizing optical

⁶ Author to whom any correspondence should be addressed.

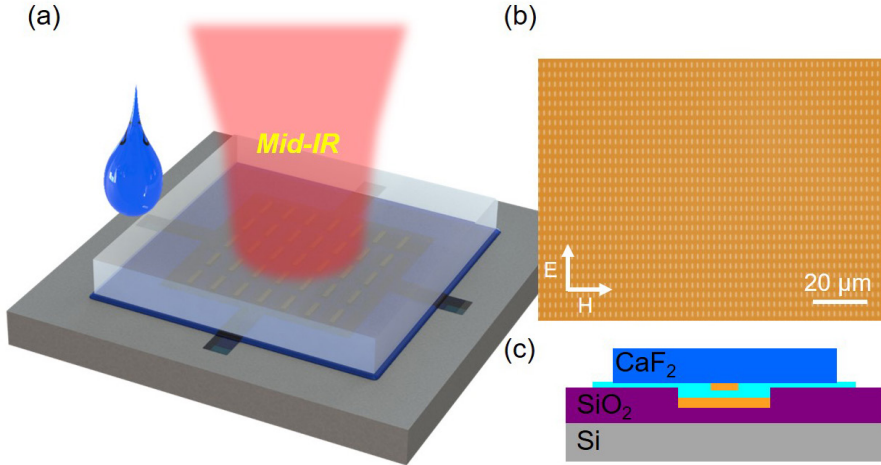


Figure 1. Illustration of the (a) capillary driven MIR plasmonic sensor. (b) Optical microscopic images of the fabricated plasmonic resonators on CaF_2 substrate. (c) Cross-sectional drawing of the capillary driven MIR plasmonic sensor.

waveguide which can strongly confine and guide light to provide long sensing path [14–16]. In particular, subwavelength photonic structures are investigated to enhance light–matter interaction [17–20]. The other solution is employing plasmonic metasurfaces to concentrate light beyond the optical diffraction limit so that high electric field intensity can be achieved. Plasmonic metasurfaces have been reported to enhance the sensing capability of MIR spectroscopy utilizing metallic nanostructures [21–24]. The highly confined electromagnetic field in the subwavelength region allows for direct interaction of a plasmonic antenna with its surrounding medium in both gas and liquid form [11, 25–27]. In other words, while the vibrational modes of molecules may not effectively interact with the incident light, they strongly couple with the plasmonic antenna, which results in a significant enhancement to the far-field spectral response. This electromagnetic response can be further tailored through engineering the geometrical configuration of the unit cell of metasurfaces [28–31].

The strong coupling between biochemical molecules and plasmonic antenna, however, is effective when they are in a close distance [32]. As a consequence, it is of high demand to develop a sensing platform which delivers biochemical molecules to specific sensitive hot-spots of the plasmonic metasurfaces. Recently, the integration of plasmonics antenna and microfluidics has been demonstrated for sensing of various biochemical materials such as chemical solutions, sugars [33], proteins [34], and lipid membranes [35]. Microfluidics is an efficient method that allows for precise manipulation of liquid and micro-substances inside fluidic channels [36–38]. Nevertheless, the large volume of aqueous solution in the micrometer scale compared to the small size of biochemical molecules in nanometer scale still leaves a distance between molecules and the plasmonic antenna [39, 40]. In addition, the strong absorption from a large volume of water could weaken the reflected/transmitted signal, and hence, hinders the sensing ability of such platform. To overcome this issue, the confinement of water samples into nano-metric spaces have been reported to study the molecule behavior [13, 41]. This significantly reduces the water absorption across the spectrum while allowing further study of unique

physics of molecules in a nano-metric scale [42–44]. More importantly, the confinement of liquid sample into nano-metric space helps to deliver biochemical molecules into direct contact with the plasmonic antenna, as most molecules are in nanometer size. However, the fabrication process, as well as a fluid controlling system of nanofluidics, is yet to be fully explored as compared to microfluidic devices.

In this work, we present a capillary-driven liquid sensor utilizing quadrupolar plasmonic resonators manipulating liquid in extremely confined space. The surface energy and silicon dioxide (SiO_2) was utilized to drive sample liquid into the sensing chamber, and hence neither external liquid pumping power nor complicated control system was required [45–47]. Simple plasmonic cut-wire resonator was designed to study the device capability fundamentally, and a metamaterial absorber configuration excited with quadrupolar resonance was introduced where the liquid sample was sandwiched in between cut-wire resonators and a metallic mirror [48–50]. When linear polarized IR light incident through cut-wire resonators with electrical field along the length, the quadrupole mode resonance is excited and strong field confinement can be seen in the sandwiched space. This induces a strong coupling between molecules and the plasmonic antenna, and thus, it is expected to enhance the IR signal. Electromagnetically induced transparency (EIT)-like response [51, 52] with a gradual change in the strength at the absorption band of the water molecule (H_2O) was observed when varied H_2O content in ethanol solution was introduced. The presented MIR plasmonic sensing platform is a potential candidate in realizing portable, non-destructive and label-free molecular analysis with high sensitivity.

2. Method

The concept of the MIR plasmonic sensing device is presented in figure 1. A sensing liquid-chamber was fabricated on SiO_2 layer thermally grown on top of intrinsic silicon (Si) substrate, and the bottom of the chamber was deposited with a reflective gold (Au) layer. A calcium fluoride (CaF_2) substrate

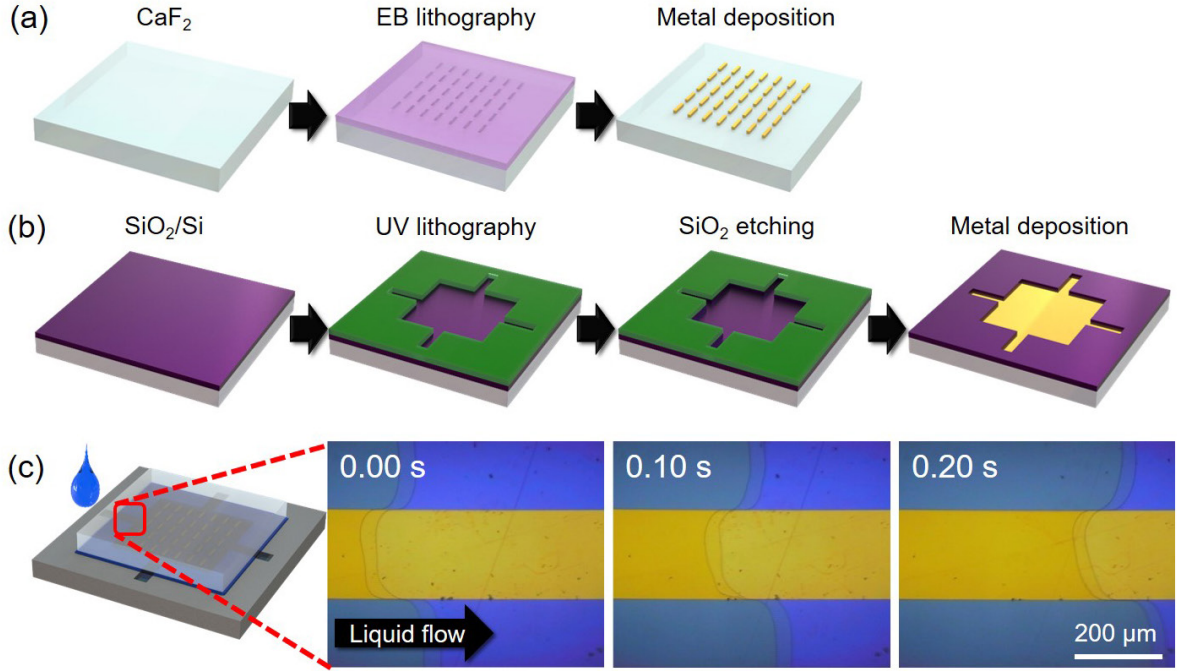


Figure 2. (a) Fabrication of cut-wire plasmonic resonators on CaF₂ substrate. (b) Fabrication process of the nano-metric chamber with reflective Au mirror. (c) Microscopic images of sample introduction area utilizing capillary force.

patterned with Au plasmonic resonators was pressed against the liquid-chamber chip and fixed with Kapton tape leaving space for the liquid sample to flow in. The Si liquid-chamber chip was diced larger than the CaF₂ chip, and thus, sample introduction was performed through simple action by placing liquid droplet at the edge of CaF₂ chip. Capillary force in the confined space drove liquid sample into the sensing chamber, and thus the liquid sample was sandwiched in between the bottom reflector of the chamber and the plasmonic resonators. The incident IR radiation was polarized along the length of the cut-wire resonator so to excite the quadrupole resonance, and the reflected MIR spectral information was observed and analyzed.

Figures 2(a) and (b) illustrate the fabrication process of the presented plasmonic resonator and the chamber chip respectively. The plasmonic resonators were patterned on a 500 μm thick CaF₂ substrate in a 250 μm² area using electron beam (EB) lithography, following by chromium (Cr)/Au evaporation at 5 nm/60 nm (figure 2(a)). On the other hand, the chamber chip was fabricated on 625 μm thick Si substrate with 300 nm thick SiO₂ on top. As illustrated in figure 2(b), ultraviolet (UV) lithography was performed to pattern the chamber area on the SiO₂ surface. A cross mark was designed for easier alignment of the resonator area on CaF₂ substrate and the Au mirror area on Si substrate. The etching process of the surface SiO₂ layer was then conducted to create a hollow chamber using reactive ion etching, following by Cr/Au deposition to create reflective mirror structure at the chamber bottom. The depth of the Au reflective chamber was measured to be 111 nm using atomic force microscopy (AFM). In order to study the absorber effect, we have fabricated a nano-metric chamber without an Au mirror. The depth of this

non-reflective (NR) chamber contains a 104 nm deep sensing area with a 196 nm thick SiO₂ layer at the bottom supported by Si substrate. Both reflective and non-reflective chamber were treated with oxygen (O₂) plasma to enhance their hydrophilicity and to remove contamination in order to make smooth contact of CaF₂ and SiO₂ surface prior to the bonding process. Figure 2(c) shows the microscopic images of liquid flow at the cross-mark area after dropping liquid sample. It is observed that liquid flowed smoothly into the nano-metric chamber, while water-SiO₂ interface moves faster than that of water-Au interfaces as shown in figure 2(c). This indicates the fact that, despite the relative hydrophobicity of Au presenting after O₂ plasma treatment, the hydrophilicity of the SiO₂ surface can strongly drive the liquid to flow into the sensing chamber.

Plasmonic cut-wire resonator was utilized for quantitative evaluation of chemicals. The simulation was first carried out to design plasmonic resonators using Lumerical finite-difference time domain (FDTD) solution. A unit cell of plasmonic nanorod antenna with periodic boundary condition is used to optimize plasmonic behavior in the designed system. The length of the cut-wire antenna was designed at 1.75 μm so to achieve strong resonance at around 2000 cm⁻¹, which is expected to redshift when the aqueous solution is introduced because of its higher refractive index. The width of the antenna was optimized at 0.28 μm in order to achieve strong resonance. When no chamber is applied to the CaF₂ plasmonic substrate, a bipolar resonance peak from the plasmonic antenna was obtained, which also indicates the high transparency of CaF₂ substrate in the IR spectral region (figure 3(b)). A resonance dip was seen when applying of non-reflective chamber caused by the partial reflection of SiO₂/Si substrate. In contrast, a much sharper resonance dip was seen using the

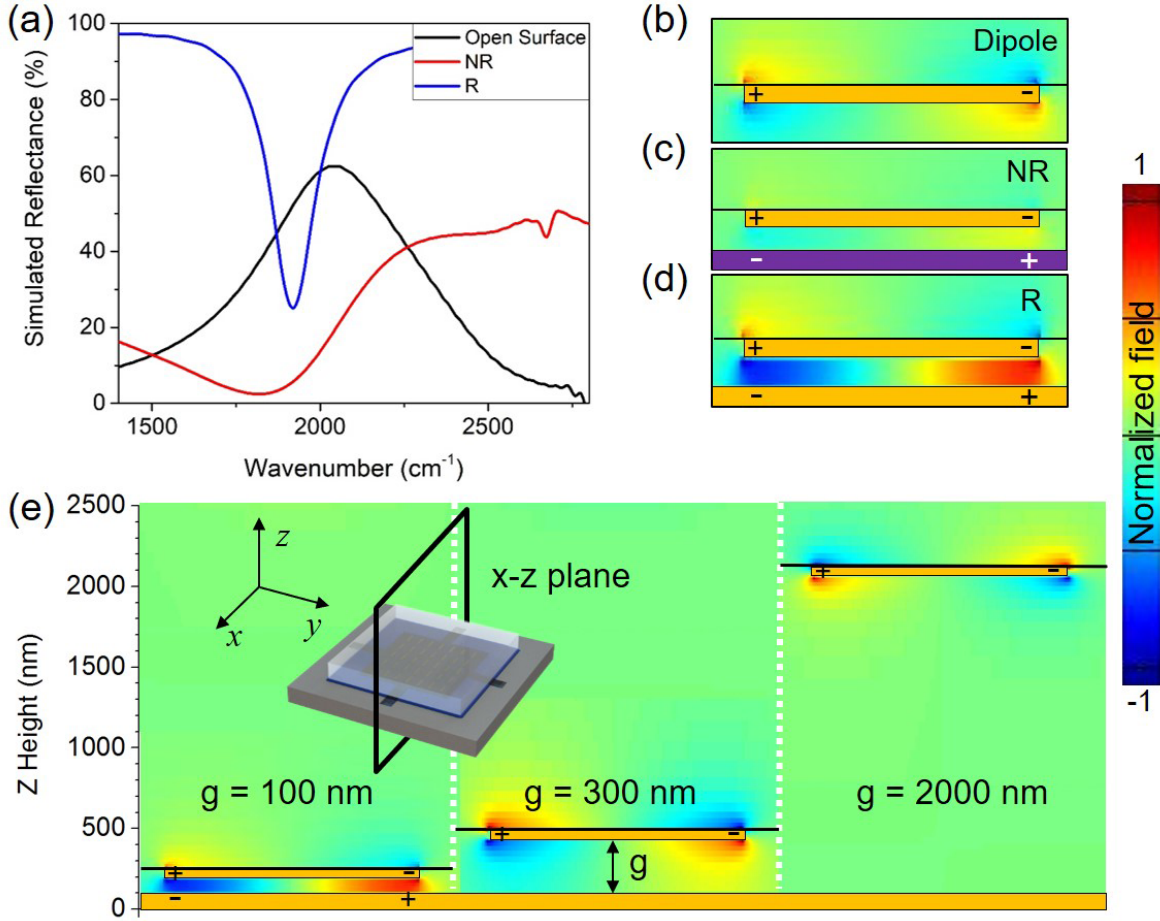


Figure 3. (a) Simulated reflected MIR spectra of plasmonic antenna fabricated on CaF₂ without the nano-metric chamber, and with the nano-metric chamber of SiO₂ (NR) and Au (R) bottom layer. Simulated electrical field distribution at the Z direction of the (b) bipolar resonance and quadrupole resonance with (c) SiO₂ (NR) and (d) Au (R) bottom layer. (e) Simulated electrical field distribution along Z direction with the Au mirror at varied gap height.

reflective Au chamber. As presented in figures 3(c) and (d), inverted electrical field distribution was excited at the bottom of both non-reflective and reflective chamber, and quadrupole resonances were formed. Nevertheless, reflective Au chamber significantly enhanced the electrical field intensity in the nano-metric space by 1 order of magnitude compared to the SiO₂/Si substrate. When comparing simple dipole resonance with reflective quadrupole resonance, intensive electrical field confinement at the nanogap was seen. Hence, this electrical field enhancement forms a nanogap hot-spot which is expected to enable higher sensitivity. Figure 3(e) presents the resonance mode variation at different gap height. When the gap was at 100 nm, quadrupolar mode dominated, because the cut-wire antenna formed a stable state with the mirror. In contrast, when the cut-wire antenna and the mirror were at larger distance, bipolar mode dominated, and no interaction between the electrical field of the cut-wire antenna and the mirror was observed. It is important to note that the reflected signal was still enhanced by the mirror in case of larger gap distance. Hence, a mirror structure allows for signal enhancement while a narrower gap height at nanometer scale may confine and enhance the electrical field at the sensing space.

3. Results and discussion

Figure 4 presents the AFM image (figure 4(a)) and the measured Fourier transform infrared (FTIR) spectra (figure 4(b)) of the fabricated devices. The width and length of the fabricated plasmonic cut-wire were 0.28 μm and 1.75 μm respectively, and the horizontal and lateral pitch of the cut-wire array were 2.0 μm and 3.5 μm. Fabrication error of 0.05 μm to 0.08 μm from the designed geometric parameter was measured, which can be due to the limited writing resolution of the EB lithography as well as metal lift-off process. During the FTIR measurement, the electrical field of the incident MIR radiation was linearly polarized along the length of the plasmonic resonators. Similar to the simulation results presented in figure 3(a), a stronger resonance is experimentally observed when applying liquid-chamber with Au mirror (figure 3(b)). It should be noted that molecular vibration of carbon dioxide (CO₂) molecule in the atmosphere was also observed in the obtained spectra, which can be eliminated through introduction of a closed sensing chamber.

We first compare the spectral responses of both non-reflective and reflective liquid-chamber using plane CaF₂ cover without plasmonic resonators. Broadband Agilent FTIR

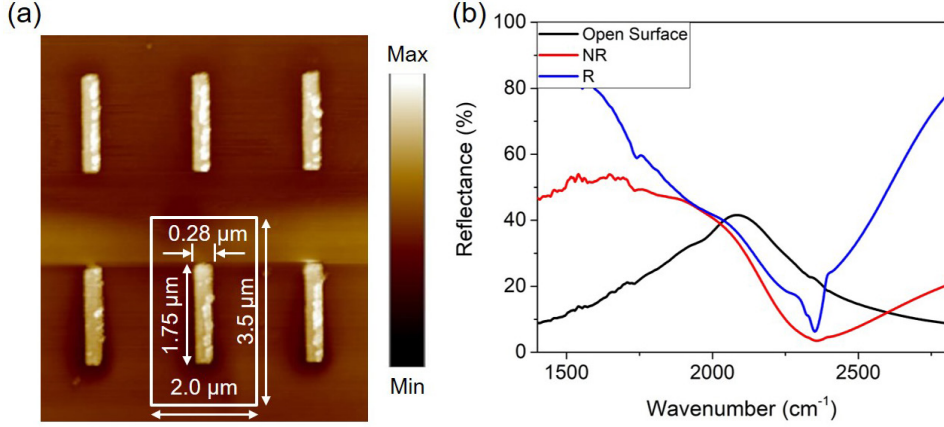


Figure 4. (a) Atomic force microscopy (AFM) image of the fabricated plasmonic resonators with geometrical parameters. (b) Measured reflected MIR spectra of plasmonic antenna fabricated on CaF_2 without nano-metric chamber, and with nano-metric chamber of SiO_2 (NR) and Au (R) bottom layer.

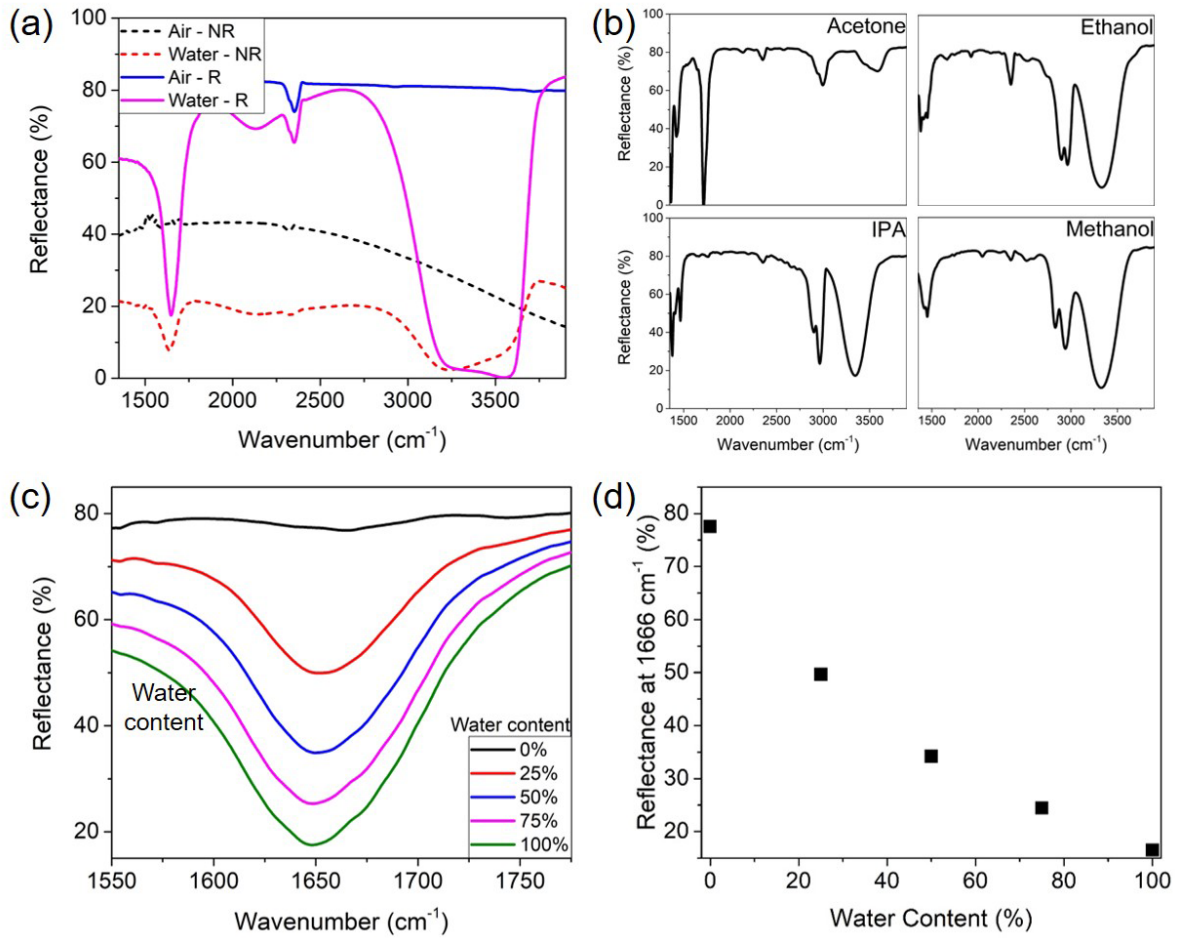


Figure 5. (a) Measured reflected MIR spectra of water and air in liquid-chamber with SiO_2 (NR) and Au (R) bottom layer. (b) Measured reflected MIR spectra of acetone, ethanol, isopropyl alcohol (IPA), and methanol using the capillary force driven into liquid-chamber. (c) Measured reflected IR spectra of water/ethanol mixture with varied water content. (d) The reflectance at 1666 cm^{-1} vibrational mode of water plotted against its concentration in water/ethanol mixture.

spectroscopy system was used to obtain the normalized reflection spectra of the fabricated plasmonic antenna, with an aperture size of $200 \mu\text{m}$ square. The reflectance of the measured spectra was normalized with respect to that of a smooth Au surface, and the sampling resolution was fixed at 4 cm^{-1} . Each

spectrum was obtained through an average of 32 scan samples. As shown in figure 5(a), it is apparent that strong spectral response from H_2O sample can be obtained using the reflective Au chamber, compared the non-reflective chamber. The reflective Au layer enhanced the observed spectral contrast

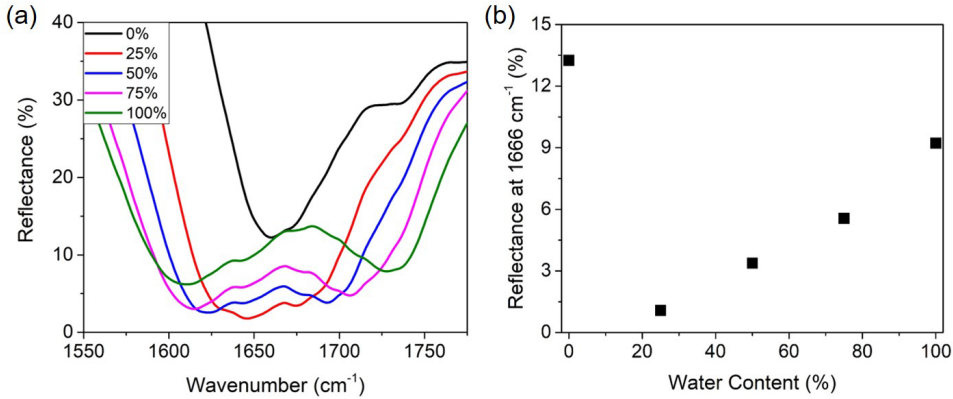


Figure 6. (a) Measured reflected MIR spectra of water/ethanol mixture with varied water content using Au plasmonic resonators. (b) The reflectance at 1666 cm^{-1} plotted against its concentration in water/ethanol mixture.

at the vibrational modes of H_2O molecule for 47% around 3333 cm^{-1} and 20% at 1666 cm^{-1} . The reflected spectra of common alcoholic liquids were also obtained as presented in figure 5(b) where the unique vibrational modes of their chemical bonds were clearly observed. The large spectral contrast at the vibrational mode enables quantitative evaluation of liquid. We measured the reflected spectra from liquid H_2O /ethanol mixture (figure 5(c)) and plotted the value of reflectance at 1666 cm^{-1} against the H_2O content in figure 5(d). Pure ethanol does not absorb MIR radiation at 1666 cm^{-1} , and hence a high reflectance at 77.5% was observed. This value gradually decreased as the water content increased and reached the smallest of 16.5% with pure H_2O sample.

The molecular fingerprint sensing capability of the fabricated devices was then examined through obtaining reflection spectra with varied water content in an ethanol solution, as presented in figure 6(a). In pure ethanol solution, a resonance dip is observed at 1666 cm^{-1} , which can be attributed to the light absorption by the cut-wire resonator. The higher refractive index of ethanol compared to air has caused the redshift. When the water content is increased to 25%, an enhancement of the resonance can be observed at 1666 cm^{-1} where the water molecular vibrational mode exhibits as described in figure 3(a). As the water content further increased, a sharp increase of the reflectance value at 1666 cm^{-1} is observed. This drastic change in the reflectance spectrum shows the coupling between the plasmonic resonance and the vibrational mode of water molecules which presents an EIT-like response [51, 52]. The reflectance value of each spectrum at 1666 cm^{-1} was plotted against the water content in figure 6(b). Larger amount of water content induced a stronger coupling between the plasmonic resonators and water molecules, and hence, the designed device is capable in quantitative sensing specifically targeted at the vibrational mode of water at 1666 cm^{-1} . Selective and quantitative sensing of specific molecule was demonstrated. Optimization of the bonding process is required to assure formation of nanometric sensing space at high reproducibility for practical applications. More complex micro/nanofluidic configuration may also be included using

CMOS (complementary metal-oxide-semiconductor) compatible materials [53–55]. Through further optimization of the materials, process, and measurement condition, a sensing platform for advanced sensing applications may be achieved.

4. Conclusion

In conclusion, a capillary driven sensing platform utilizing MIR plasmonic resonators for specific chemicals in aqueous environment was proposed. We fabricated nano-metric chamber chip with Au mirror at the bottom forming a metamaterial absorber configuration which could support quadrupolar resonance inside the chamber. Through forming a nano-metric space using hydrophilic SiO_2 , capillary effect can be utilized to draw liquid into the sensing area. The enhancement of the molecular vibrational mode as well as the plasmonic resonators were clearly seen individually through experimental and simulation demonstration. The coupling between the molecule and the plasmonic resonators was further observed through the mixture analyte of water and ethanol. Quantitative evaluation of water/ethanol mixture was achieved using the cut-wire resonators specifically designed to couple with a vibrational mode of water molecule around at 1666 cm^{-1} . Through further process development, capillary force driven fluidics devices integrated with plasmonic resonators may become an ideal tool in analyzing biochemical samples. Furthermore, the optimization of the plasmonic resonator design and selective functionalization of molecules on resonators may realize selective detection of biochemical molecules with much higher sensitivity in near future.

Acknowledgment

The authors acknowledge the financial support from the research grant of NRF-CRP15-2015-02 and NRF2015-NRF-ISF001-2620 NUS at the National University of Singapore (NUS); and partially supported by the National Natural Science Foundation of China under Grant No. 61474078 at NUS (Suzhou) Research Institute, Suzhou, China.

ORCID iDs

Chengkuo Lee  <https://orcid.org/0000-0002-8886-3649>

References

- [1] Fan X, White I M, Shopova S I, Zhu H, Suter J D and Sun Y 2008 Sensitive optical biosensors for unlabeled targets: a review *Anal. Chim. Acta* **620** 8–26
- [2] Freudiger C W, Min W, Saar B G, Lu S, Holtom G R, He C, Tsai J C, Kang J X and Xie X S 2008 Label-free biomedical imaging with high sensitivity by stimulated Raman scattering microscopy *Science* **322** 1857–61
- [3] Tonouchi M 2007 Cutting-edge terahertz technology *Nat. Photon.* **1** 97
- [4] Adato R and Altug H 2013 *In situ* ultra-sensitive infrared absorption spectroscopy of biomolecule interactions in real time with plasmonic nanoantennas *Nat. Commun.* **4** 2154
- [5] Baker M J et al 2014 Using Fourier transform IR spectroscopy to analyze biological materials *Nat. Protocols* **9** 1771
- [6] Khalil M, Demirdöven N and Tokmakoff A 2003 Coherent 2D IR spectroscopy: molecular structure and dynamics in solution *J. Phys. Chem. A* **107** 5258–79
- [7] Hu T, Dong B, Luo X, Liow T-Y, Song J, Lee C and Lo G-Q 2017 Silicon photonic platforms for mid-infrared applications [invited] *Photonics Res.* **5** 417–30
- [8] Zou Y, Chakravarty S, Chung C-J, Xu X and Chen R T 2018 Mid-infrared silicon photonic waveguides and devices [Invited] *Photonics Res.* **6** 254–76
- [9] Rodrigo D et al 2018 Resolving molecule-specific information in dynamic lipid membrane processes with multi-resonant infrared metasurfaces *Nat. Commun.* **9** 2160
- [10] Adato R, Yanik A A, Amsden J J, Kaplan D L, Omenetto F G, Hong M K, Erramilli S and Altug H 2009 Ultra-sensitive vibrational spectroscopy of protein monolayers with plasmonic nanoantenna arrays *Proc. Natl Acad. Sci.* **106** 19227–32
- [11] Chang Y, Hasan D, Dong B, Wei J, Ma Y, Zhou G, Ang K W and Lee C 2018 All-dielectric surface-enhanced infrared absorption-based gas sensor using guided resonance *ACS Appl. Mater. Interfaces* **10** 38272–9
- [12] Lin P T, Lin H-Y G, Han Z, Jin T, Millender R, Kimerling L C and Agawal A 2016 Label-free glucose sensing using chip-scale mid-infrared integrated photonics *Adv. Opt. Mater.* **4** 5
- [13] Le T H H and Tanaka T 2017 Plasmonics–nanofluidics hybrid metamaterial: an ultrasensitive platform for infrared absorption spectroscopy and quantitative measurement of molecules *ACS Nano* **11** 9780–8
- [14] Dong B, Guo X, Ho C P, Li B, Wang H, Lee C, Luo X and Lo G 2017 Silicon-on-insulator waveguide devices for broadband mid-infrared photonics *IEEE Photonics J.* **9** 1–10
- [15] Dong B et al 2019 Aluminum nitride on insulator (AlNOI) platform for mid-infrared photonics *Opt. Lett.* **44** 73–6
- [16] Dong B, Luo X, Hu T, Guo T X, Wang H, Kwong D, Lo P G and Lee C 2018 Compact low loss mid-infrared wavelength-flattened directional coupler (WFDC) for arbitrary power splitting ratio enabled by rib waveguide dispersion engineering *IEEE J. Sel. Top. Quantum Electron.* **24** 1–8
- [17] Dong B, Hu T, Luo X, Chang Y, Guo X, Wang H, Kwong D-L, Lo G-Q and Lee C 2018 Wavelength-flattened directional coupler based mid-infrared chemical sensor using bragg wavelength in subwavelength grating structure *Nanomaterials* **8** 893
- [18] Ma Y, Dong B, Li B, Ang K-W and Lee C 2018 Dispersion engineering and thermo-optic tuning in mid-infrared photonic crystal slow light waveguides on silicon-on-insulator *Opt. Lett.* **43** 5504–7
- [19] Wei J, Sun F, Dong B, Ma Y, Chang Y, Tian H and Lee C 2018 Deterministic aperiodic photonic crystal nanobeam supporting adjustable multiple mode-matched resonances *Opt. Lett.* **43** 5407–10
- [20] Ma Y, Dong B, Li B, Wei J, Chang Y, Ho C P and Lee C 2018 Mid-infrared slow light engineering and tuning in 1D grating waveguide *IEEE J. Sel. Top. Quantum Electron.* **24** 1–8
- [21] Anker J N, Hall W P, Lyandres O, Shah N C, Zhao J and Van Duyne R P 2008 Biosensing with plasmonic nanosensors *Nat. Mater.* **7** 442
- [22] Kabashin A V, Evans P, Pastkovsky S, Hendren W, Wurtz G A, Atkinson R, Pollard R, Podolskiy V A and Zayats A V 2009 Plasmonic nanorod metamaterials for biosensing *Nat. Mater.* **8** 867
- [23] Hasan D, Ho C P, Pitchappa P, Yang B, Yang C and Lee C 2016 Thermoplasmonic study of a triple band optical nanoantenna strongly coupled to mid IR molecular mode *Sci. Rep.* **6** 22227
- [24] Hasan D and Lee C 2018 Hybrid metamaterial absorber platform for sensing of CO₂ gas at Mid-IR *Adv. Sci.* **5** 1700581
- [25] Im H, Shao H, Park Y I, Peterson V M, Castro C M, Weissleder R and Lee H 2014 Label-free detection and molecular profiling of exosomes with a nano-plasmonic sensor *Nat. Biotechnol.* **32** 490
- [26] Huck C, Neubrech F, Vogt J, Toma A, Gerbert D, Katzmajn J, Härtling T and Pucci A 2014 Surface-enhanced infrared spectroscopy using nanometer-sized gaps *ACS Nano* **8** 4908–14
- [27] Dregely D, Neubrech F, Duan H, Vogelgesang R and Giessen H 2013 Vibrational near-field mapping of planar and buried three-dimensional plasmonic nanostructures *Nat. Commun.* **4** 2237
- [28] Pitchappa P, Ho C P, Dhakar L and Lee C 2015 Microelectromechanically reconfigurable interpixelated metamaterial for independent tuning of multiple resonances at terahertz spectral region *Optica* **2** 571–8
- [29] Zheludev N I and Kivshar Y S 2012 From metamaterials to metadevices *Nat. Mater.* **11** 917
- [30] Ma F, Qian Y, Lin Y-S, Liu H, Zhang X, Liu Z, Tsai J M-L and Lee C 2013 Polarization-sensitive microelectromechanical systems based tunable terahertz metamaterials using three dimensional electric split-ring resonator arrays *Appl. Phys. Lett.* **102** 161912
- [31] Shih K, Pitchappa P, Manjappa M, Ho C P, Singh R, Yang B, Singh N and Lee C 2017 Active MEMS metamaterials for THz bandwidth control *Appl. Phys. Lett.* **110** 161108
- [32] John-Herpin A, Tittl A and Altug H 2018 Quantifying the limits of detection of surface-enhanced infrared spectroscopy with grating order-coupled nanogap antennas *ACS Photonics* **5** 4117–24
- [33] Mesch M, Zhang C, Braun P V and Giessen H 2015 Functionalized hydrogel on plasmonic nanoantennas for noninvasive glucose sensing *ACS Photonics* **2** 475–80
- [34] Sreekanth K V, Alapan Y, ElKabbash M, Ilker E, Hinczewski M, Gurkan U A, De Luca A and Strangi G 2016 Extreme sensitivity biosensing platform based on hyperbolic metamaterials *Nat. Mater.* **15** 621
- [35] Limaj O, Etezadi D, Wittenberg N J, Rodrigo D, Yoo D, Oh S-H and Altug H 2016 Infrared plasmonic biosensor for real-time and label-free monitoring of lipid membranes *Nano Lett.* **16** 1502–8
- [36] Whitesides G M 2006 The origins and the future of microfluidics *Nature* **442** 368
- [37] Shih K, Pitchappa P, Manjappa M, Ho C P, Singh R and Lee C 2017 Microfluidic metamaterial sensor: selective

- trapping and remote sensing of microparticles *J. Appl. Phys.* **121** 023102
- [38] Li X, Soler M, Szydzik C, Khoshmanesh K, Schmidt J, Coukos G, Mitchell A and Altug H 2018 Label-free optofluidic nanobiosensor enables real-time analysis of single-cell cytokine secretion *Small* **14** 1800698
- [39] Mijatovic D, Eijkel J C T and van den Berg A 2005 Technologies for nanofluidic systems: top-down versus bottom-up-a review *Lab Chip* **5** 492–500
- [40] Shirai K, Mawatari K and Kitamori T 2013 Extended nanofluidic immunochemical reaction with femtoliter sample volumes *Small* **10** 1514–22
- [41] Le T H H, Morita A, Mawatari K, Kitamori T and Tanaka T 2018 Metamaterials-enhanced infrared spectroscopic study of nanoconfined molecules by plasmonics–nanofluidics hybrid device *ACS Photonics* **5** 3179–88
- [42] Xu Y, Matsumoto N, Wu Q, Shimatani Y and Kawata H 2015 Site-specific nanopatterning of functional metallic and molecular arbitrary features in nanofluidic channels *Lab Chip* **15** 1989–93
- [43] Xu Y 2018 Nanofluidics: a new arena for materials science *Adv. Mater.* **30** 1702419
- [44] Shih K, Pitchappa P, Jin L, Chen C-H, Singh R and Lee C 2018 Nanofluidic terahertz metasensor for sensing in aqueous environment *Appl. Phys. Lett.* **113** 071105
- [45] Kuo J-N and Wang W-K 2015 Capillary filling speed of ferrofluid in hydrophilic microscope slide nanochannels *Microfluidics Nanofluidics* **18** 57–64
- [46] Juncker D, Schmid H, Drechsler U, Wolf H, Wolf M, Michel B, de Rooij N and Delamarche E 2002 Autonomous microfluidic capillary system *Anal. Chem.* **74** 6139–44
- [47] Zimmermann M, Schmid H, Hunziker P and Delamarche E 2007 Capillary pumps for autonomous capillary systems *Lab Chip* **7** 119–25
- [48] Hwang I, Yu J, Lee J, Choi J-H, Choi D-G, Jeon S, Lee J and Jung J-Y 2018 Plasmon-enhanced infrared spectroscopy based on metamaterial absorbers with dielectric nanopedestals *ACS Photonics* **5** 3492–8
- [49] Liu N, Mesch M, Weiss T, Hentschel M and Giessen H 2010 Infrared perfect absorber and its application as plasmonic sensor *Nano Lett.* **10** 2342–8
- [50] Neubrech F, Pucci A, Cornelius T W, Karim S, García-Etxarri A and Aizpurua J 2008 Resonant plasmonic and vibrational coupling in a tailored nanoantenna for infrared detection *Phys. Rev. Lett.* **101** 157403
- [51] Adato R, Artar A, Erramilli S and Altug H 2013 Engineered absorption enhancement and induced transparency in coupled molecular and plasmonic resonator systems *Nano Lett.* **13** 2584–91
- [52] Krivenkov V, Goncharov S, Nabiev I and Rakovich Y P 2019 Induced transparency in plasmon–exciton nanostructures for sensing applications *Laser Photonics Rev.* **13** 1800176
- [53] Baldassarre L, Sakat E, Frigerio J, Samarelli A, Gallacher K, Calandrini E, Isella G, Paul D J, Ortolani M and Biagioni P 2015 Midinfrared plasmon-enhanced spectroscopy with germanium antennas on silicon substrates *Nano Lett.* **15** 7225–31
- [54] Barho Franziska B, Gonzalez-Posada F, Milla M-J, Bomers M, Cerutti L, Tournié E and Taliercio T 2017 Highly doped semiconductor plasmonic nanoantenna arrays for polarization selective broadband surface-enhanced infrared absorption spectroscopy of vanillin *Nanophotonics* **24** 507
- [55] Perro A, Lebourdon G, Henry S, Lecomte S, Servant L and Marre S 2016 Combining microfluidics and FT-IR spectroscopy: towards spatially resolved information on chemical processes *React. Chem. Eng.* **1** 577–94